Stability of Railroad Tracks under the Effects of Temperature Change and Earthquake

F. Arbabi[1*] and M. Khalighi[2]

1. Professor, International Institute of Earthquake Engineering and Seismology (IIEES), Tehran, Iran,
* Corresponding Author; email: farbabi@mtu.edu
2. PhD Candidate, International Institute of Earthquake Engineering and Seismology (IIEES), Tehran, Iran

ABSTRACT

One of the major causes of train accidents is derailment due to axial or lateral buckling of the track. This problem is more prominent in continuously welded rails (CWR), which are now very common because of their advantages of reduced noise and damage and more comfortable rides. As for the effect of earthquakes on track buckling, the axial force they induce seems to be much less than that of temperature change as well as those caused by tractive action and braking of locomotives. This does not mean that earthquakes cannot have a detrimental effect on railroad tracks. Their main cause of damage is the large reduction they may produce in the lateral resistance of ballast due to shaking of the ballast bed. This paper deals with the problem of axial and lateral buckling of CWR and the effects of earthquakes and temperature change on the stability of the track. A three-dimensional macro-element is used to model the track. A program, developed in Mathcad environment, is used to conduct a series of parametric studies. The results show that the simple sinusoidal form often used for determining buckling loads of tracks is only valid for totally homogeneous tracks, a rather rare situation. It was ascertained that the buckled shapes observed in practice are due to local inhomogeneities of the track.

Keywords:
Railroad; Buckling;
Energy Methods;
Finite Element Method;
Macro-element;
Earthquake

1. Introduction

The advent of replacing jointed rails with continuously welded rails (*CWR*) has had the beneficial effect of reducing the noise and vibration and increasing the life of the track as well as comfort of the passengers. It has also had an adverse effect of increasing the likelihood of buckling. A survey of track-related accidents [1] from 1976 to 1980 shows a rate of about 4000 per year. A large number of these accidents have been due to track instability. Stability of *CWR* tracks is highly affected by [2-6] loads (thermal, vehicle and earthquake) and by the reduction of lateral resistance due to lack of maintenance or other causes. In this regard, the most detrimental effect of earthquakes on railroad tracks seems to be the substantial reduction they can cause in the lateral resistance of the ballast.

At temperatures much above the neutral temperature (at which the track was laid), high compressive axial forces may develop [3] in the rails. The axial forces may also increase because of the tractive forces and braking of locomotives. These forces may cause the track to shift in the lateral direction and produce track irregularity. Should the axial force reach a critical value, the track could lose its stability. This instability may be in the form of axial or lateral-torsional buckling. A combination of vehicle loads and reduced lateral resistance of the track (e.g. due to earthquake) added to high thermal forces can exacerbate [4-5] the situation and become a cause for instability. If the strength of the track can be evaluated against instability, a maintenance program can be instituted accordingly. That is, maintenance can be performed before resistance is reduced to a critical value.

In view of the various parameters affecting it, buckling of railroad tracks can be a complex

problem. Most studies have restricted the deformation of the track to either vertical or horizontal plane, assuming one dominant buckling mode [7]. Kerr [2-3] has presented theoretical analyses of track buckling using a beam-like model. Such classical models of course lack versatility and cannot model local effects, such as missing ties, fasteners or the effect of locally untamped ballast [8]. Kish et al [9-10] and Samavedam and co-workers have published [11-13] a series of articles dealing with track buckling with a beam model. Their model does not consider the effects of non-uniformly distributed ballast resistance along the track and loss of ties or fasteners. Hengstum and Esveld [14] investigated track stability in tight curves using finite elements with a beam model. A uniaxial three-dimensional finite element model [15] was used by El-Ghazaly et al. Their approach includes the interaction between lateral and torsional buckling modes. Jackson [16] and Ramesh [17] used a two-dimensional rail-tie model to investigate lateral buckling of tracks. Lim et al [7-8] developed a three-dimensional CWR track model which was used in a nonlinear finite element program. The influence of lateral and longitudinal ballast resistance, effects of track irregularities (misalignment, gauge irregularity, etc.) were investigated [8] in a separate study.

Studies, such as those mentioned above, can be placed in two categories; one-dimensional elements with a classical or finite element analysis, or two- and three-dimensional models of a limited segment of the track. Since instability is mostly a global phenomenon, a realistic study must incorporate a large length of the track with sufficient details. The present paper uses a three-dimensional macro-element [18] to model the track. This approach will provide detailed information about the behavior of the track while at the same time not being unusually tedious in terms of time and efforts of the analysis. The first part of the paper deals with the derivation of the governing equations for the macro element. An energy approach is used in the derivation. The equilibrium equations of the problem are obtained by setting the first variation of the total energy of the system equal to zero. The elastic and geometric stiffness matrices for both axial as well as lateral buckling of the track are determined as part of the process. Some case studies are presented to show the performance of this element, and a number of parametric studies are performed to determine the behavior of railroad tracks. The methodology developed in this study includes all the major parameters of railroad tracks, as well as warping of the rails, and can be used to investigate all aspects of the problem. One exception is the exclusion of the effect of shear transfer between the sections of ballast. This was investigated by a separate three-dimensional finite element model and was judged insignificant.

2. Governing Equations

In order to keep the number of elements needed for a comprehensive study manageable, a macro element was developed and used in this study. Figure (1) shows the details of the macro element. The axis of the track is in the x-direction, and its cross section is in the y-z plane. The displacements in the x-, y- and z-directions are denoted by u, v and w. β is the rotation about the x-axis due to torsion. The degrees of freedom at each node include six generalized displacements (three displacements and three rotations). An additional degree of freedom depicts warping of the section. Torsional and lateral resistances of the ballast and the ties are represented by distributed springs with stiffness k_1 and k_2, while k_3 denotes the vertical resistance of the ballast and the subgrade.

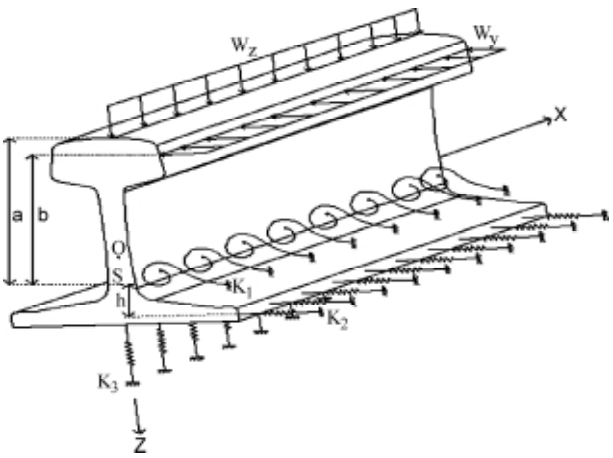

Figure 1. Macroelement for modeling the track.

The total energy of the system, Π, is the sum of the elastic energy of the resisting elements and the potential energy of the loads

$$\Pi = U_e + U_s + V_P + V_W \quad (1)$$

In Eq. (1) the elastic energy of the system is divided into two parts; the elastic energy of the rail, U_e and that of the support system (ballast, ties, fasteners and subgrade), U_s. The potential energy of the loads is also divided into two parts; the potential energy of the axial load, V_p and that of the lateral loads, V_w. Since our main concern is instability, the secondary effects of the loads must be included in the formulation. Thus, the expressions [19] for the different energy terms are as follows:

$$U_e = \frac{1}{2}\int_0^l (EAu'^2 + EI_z v''^2 + EI_y w''^2 + GJ\beta'^2 + EI\beta''^2)\,dx \tag{2}$$

Here E is the modulus of elasticity of the rail, G its shear modulus, I_y and I_z its moments of inertia about y- and z-axes, J is torsion constant. The last term in Eq. (2) is due to warping of the section, to account for warping of the thin portions of the rail section. Due to warping, parts of the section can get distorted, undergoing a displacement in the x-direction. Warping is a function of derivative of the rotation, β, with respect to x. The elastic energy associated with torsional, lateral and vertical resistances of the ties, fasteners, ballast and subgrade is:

$$U_s = \frac{1}{2}\int_0^l (k_1\beta^2 + k_2(v - h\beta)^2 + k_3 w^2)\,dx = \frac{1}{2}\int_0^l \left[k_2 v^2 + k_3 w^2 + (k_1 + k_2 h^2)\beta^2 - 2k_2 hv\beta\right]dx \tag{3}$$

The second term in the above expression indicates that lateral resistance of the track acts at or near the bottom of the rail, at a distance h from the shear center. The potential energy of the axial load, P, is:

$$V_P = -\frac{1}{2}\int_0^l P\left[v'^2 + 2(z_0 + e)v'\beta' + \int_0^l \left(\frac{I_p}{A} + e\frac{X}{I_y}\right)\beta'^2 + w'^2 + 2u\right]dx \tag{4}$$

In Eq. (4), the term $X = 2z_0 I_y - \int_A z(y^2 + z^2)\,dA$ is a property of the track section. For sections that are symmetric with respect to the y-axis, X vanishes. In the last equation z_0 is the coordinate of the shear center, S. I_p is the polar moment of inertia and A is the area of the cross-section of the rail. The eccentricity of the axial load, e, is positive when the load is above the centroid. W_z, and W_y are the vertical and horizontal loads, acting at distances a and b (in the vertical direction) from the shear center. The potential energy of lateral loads [20] consists of two parts. The first part, V_{w1}, is the product of the applied loads and their corresponding displacements. The changes in the potential energy due to flexural and torsional actions are incorporated in the second part, V_{w2}.

$$V_w = V_{w1} + V_{w2} \tag{5}$$

where

$$V_{w1} = -\int_0^l \left[W_z \cdot w + W_y(v + b\beta)\right]dx - (Q_{y1}v_1 + Q_{y2}v_2 + Q_{z1}w_1 + Q_{z2}w_2 + M_{y1}w'_1 + M_{y2}w'_2 + M_{z1}v'_1 + M_{z2}v'_2) + M_x(\beta_1 - \beta_2)$$

and

$$V_{w2} = \frac{1}{2}\left[Q_{y1}\int_0^l w''\beta x\,dx + Q_{y2}\int_0^l w''\beta(l - x)\,dx + Q_{z1}\int_0^l v''\beta x\,dx + Q_{z2}\int_0^l v''\beta(l - x)\,dx + M_{y1}\int_0^l v''\beta\,dx + M_{y2}\int_0^l v''\beta\,dx + M_{z1}\int_0^l w''\beta\,dx + M_{z2}\int_0^l w''\beta\,dx + \frac{1}{2}W_z\int_0^l v''\beta[x^2 + (l - x)^2]\,dx + W_z a\int_0^l \beta^2\,dx + \frac{1}{2}W_y\int_0^l w''\beta[x^2 + (l - x)^2]\right]dx$$

For a conservative torque the potential energy is given by

$$V_t = -\frac{1}{2}M_x\int_0^l (v'w'' - w'v'')\,dx \tag{6}$$

3. Earthquake Effects

The energy equations 2 to 6, can be used for static and stability analyses. For earthquake, studies the ground acceleration renders the problem dynamic. In that case, the right-hand side of the latter equations will have a time integral as well. The inertia forces are due to the mass of the rail, m_r and an

added mass due to other components, such as ties, tie plates and the part of the ballast, m_a, vibrating with the system. The centroid of the rail section and the center of the added mass are located at distances c and d from the shear center. Thus, for lateral motion the kinetic energy is:

$$T = \int_t \left[(m_r + m_a) \dot{v}_t^2 + (m_r c + m_a d) \dot{\beta}_t^2 \right] dt \qquad (7)$$

The subscript t indicates total displacement whose value in the lateral direction is: $v_t = v_c + v_g$ Here v_c is the lateral displacement of the centroid and v_g is that of the ground. In the derivation of the equilibrium equations the variables are expressed in terms of the values of the shear center. The relation between the latter displacements and those of the centroid are derived by various authors [21]. Substitution for v_t in Eq. (7) and then finding the equilibrium equations (Section 4), will lead to the ground acceleration as an input force. For a given earthquake, such as that of Tabas, the acceleration function can be used along with a step-by-step solution process.

4. Shape Functions and Stiffness of the Element

In order to use the displacements and rotations of the nodes as basic variables of the system, we start out expressing the displacement and rotation of an arbitrary point in the element by polynomials with a number of constant coefficients equal to that of the degrees of freedom at the two ends of the element. For the axial displacement we can write, $u = \mathbf{M}\mathbf{s}_1$. The elements of the row matrix M are $M_1 = 1 - \frac{x}{l}$, $M_2 = \frac{x}{l}$ and $\mathbf{s}_1{}^T = [u_1 \quad u_2]$. Similarly expressions for the lateral displacements and torsional rotation are $v = \mathbf{N}\mathbf{s}_2$, $w = \mathbf{N}\mathbf{s}_3$ and $\beta = \mathbf{N}\mathbf{s}_4$. The elements of the vector of shape functions, N, are $N_1 = 1 - 3\frac{x^2}{l^2} + 2\frac{x^3}{l^3}$, $N_2 = x - 2\frac{x^2}{l} + \frac{x^3}{l^2}$, $N_3 = 3\frac{x^2}{l^2} - 2\frac{x^3}{l^3}$ and $N_4 = -\frac{x^2}{l} + \frac{x^3}{l^2}$. These are the familiar Legendre polynomials. The displacement vectors are $\mathbf{s}_2{}^T = [v_1 \ \theta_{z1} \ v_2 \ \theta_{z2}]$, $\mathbf{s}_3{}^T = [w_1 \ \theta_{y1} \ w_2 \ \theta_{y2}]$ and $\mathbf{s}_4{}^T = [\theta_{x1} \ \theta'_{x1} \ \theta_{x2} \ \theta'_{x2}]$.

u_i and v_i are nodal displacements, rotations about the y- and z-axes and nodal torsional rotations. θ_{xi} are the degrees of freedom associated with warping.

Substituting the derivatives of the displacement terms in the expression for elastic energy, Eq. (2), and taking the terms that are independent of x outside the integral, results in the elastic energy in terms of the nodal displacement vectors:

$$U_e = \frac{1}{2}(s_1{}^T K_1 s_1 + s_2{}^T K_2 s_2 + s_3{}^T K_3 s_3 + s_4{}^T K_4 s_4) \quad (8)$$

where $K_1 = EA\int_0^l M'^T M' dx$ is the stiffness of the element against axial deformation. $K_2 = EI_z \int_0^l N''^T \times N'' dx$ is the stiffness matrix for deformation in the y-direction. The stiffness matrix for deformation in the z-direction, K_3, has a similar form with I_z replaced by I_y. The stiffness matrix for torsion and warping is $K_4 = \frac{GJ}{2}\int_0^l N'^T N' dx + \frac{E\Gamma}{2}\int_0^l N''^T N'' dx$. Each term of this stiffness matrix can be directly calculated from $K_{4_{ij}} = \frac{GJ}{2}\int_0^l N_i' N_j' dx + \frac{E\Gamma}{2}\int_0^l N_i'' N_j'' dx_j$.

Proceeding in a similar fashion with other energy terms, the elastic energy of the support springs, Eq. (3), yields,

$$U_s = \frac{1}{2}(s_2^T K_{s2} s_2 + s_3^T K_{s3} s_3 + s_4^T K_{s4} s_4 + s_2^T K_{s24} s_4 + s_4^T K_{s42} s_2) \qquad (9)$$

with

$$K_{s2} = k_2 \int_0^l N^T N dx,$$

$$K_{s3} = k_3 \int_0^l N^T N dx,$$

$$K_{s4} = (k_1 + k_2 h^2) \int_0^l N^T N dx,$$

$$K_{s24} = K_{s42} = -k_2 h \int_0^l N^T N dx.$$

The last term of Eq. (3) results in the last two terms of Eq. (9). This splitting of the terms is done in order to preserve the symmetry of the stiffness matrix. The potential energy of the axial load, Eq. (4), results in an expression in terms of the geometric stiffness matrices as:

$$V_P = \frac{1}{2}(s_2^T K_{g2} s_2 + s_3^T K_{g3} s_3 + s_4^T K_{g4} s_4 + s_2^T K_{g24} s_4 + s_4{}^T K_{g42} s_2 - 2 s_1{}^T P) \qquad (10)$$

with

$$K_{g2} = K_{g3} = -P\int_0^l N'^T\, N'\, dx,$$

$$K_{g4} = -P\left(\frac{I_p}{A} + e\frac{X}{I_y}\right)\int_0^l N'^T\, N'\, dx$$

and

$$K_{g24} = K_{g42} = -P(z_0 + e)\int_0^l N'^T\, N'\cdot dx$$

The potential energy of the lateral loads becomes

$$\begin{aligned} V_{w1} = &\int_0^\ell W_z w dx + \int_0^\ell W_y v dx + \int_0^\ell b W_y v + \\ &s_2{}^T W_y + s_4{}^T b W_y + Q_{y1} v_1 + Q_{y2} v_2 + \\ &Q_{z1} w_1 + Q_{z2} w_2 + M_{y1} w'_1 + M_{y2} w'_2 + \\ &M_{z1} v'_1 + M_{z2} v'_2 \end{aligned} \tag{11}$$

and

$$\begin{aligned} V_{w2} = &s_2^T K_{gw24} s_4 + s_3^T K_{gw34} s_4 + \\ &s_4^T K_{gw4} s_4 + s_2^T K_{gw23} s_3 + s_3^T K_{gw32} s_2 \end{aligned} \tag{12}$$

with

$$\begin{aligned} K_{gw24} = \frac{1}{2}\Big[&Q_{z1}\int_0^\ell N'' N x dx + Q_{z2}\int_0^\ell N'' N(l-x) dx + \\ &(M_{y1} - M_{y2})\int_0^\ell N'' N dx + \frac{1}{2} W_z \int_0^\ell N'' N \times \\ &[x^2 + (l-x)^2] dx + \quad M_x (N'N'' - N'N'') dx \Big] \end{aligned}$$

$$\begin{aligned} K_{gw34} = \frac{1}{2}\Big[&Q_{y1}\int_0^\ell N'' N x dx + Q_{y2}\int_0^\ell N'' N(l-x) dx + \\ &(M_{z1} - M_{z2})\int_0^\ell N'' N dx + \\ &\frac{1}{2} W_y \int_0^\ell N'' N[x^2 + (l-x)^2] dx \Big] \end{aligned}$$

$$K_{gw4} = \tfrac{1}{2} W_z a \int N^T N dx$$

$$K_{gw23} = \frac{M_x}{2}\int_0^\ell N'\, N''\cdot dx$$

and

$$K_{gw32} = \frac{-M_x}{2}\int_0^\ell N''\, N'\cdot dx$$

For the vertical loads the load vector, associated with the displacement vector s_3, is:

$$P_z{}^T = [\, p_z \frac{l}{2} + P_{1z} \quad p_z \frac{l^2}{12} \quad p_z \frac{l}{2} + P_{2z} \quad -p_z \frac{l^2}{12}]$$

For the loads in the *y*-direction, with displacement vectors s_2 and s_4, the terms in Eq. (11) yield

$$P_y{}^T = \left[\, p_y \frac{l}{2} + P_{1y} \quad p_y \frac{l^2}{12} \quad p_y \frac{l}{2} + P_{2y} \quad -p_y \frac{l^2}{12}\right]$$

and

$$bP_y{}^T = \left[\, bp_y \frac{l}{2} + bP_{1y} \quad bp_y \frac{l^2}{12} \quad bp_y \frac{l}{2} + bP_{2y} \quad -bp_y \frac{l^2}{12}\right]$$

Substitution of the shape functions for displacements in Eq. (7) of the kinetic energy will yield the mass matrix for the element.

5. Equilibrium Equations

The equilibrium equations for the static and stability problems can be obtained by minimizing the total energy of the system in space, i.e. by setting the first variation of the total energy equal to zero. In view of equations 6 to 9, the variation of the total energy of the system becomes:

$$\begin{aligned} &\delta s_1{}^T [K_1 s_1 - P_x] + \delta s_2{}^T [(K_2 + K_{S2} + K_{g2}) s_2 - P_y] + \\ &\delta s_3{}^T [(K_3 + K_{s3} + K_{g3}) s_3 - P_z] + \\ &\delta s_4{}^T (K_4 + K_{s4} + K_{g4} + 2K_{gw4)}) s_4 + \\ &\delta s_2{}^T [(K_{s24} + K_{g24} + K_{gw24}) s_4 + \\ &\delta s_4{}^T [(K_{s42} + K_{g42} + K_{gw42}) s_2 + \delta s_2{}^T K_{gw23} s_3 + \\ &\delta s_3{}^T K_{gw32} s_2 - \delta s_3{}^T P_z - \delta s_2{}^T P_y - \delta s_4{}^T b P_y] = 0 \end{aligned} \tag{13}$$

Since δs_i are nonzero variations, for the above identity to be satisfied, the factor of each of these variations must vanish, leading to the following equilibrium equations for the element:

$$(K_e + K_s + K_g + K_{gw}) s = S \tag{14}$$

Assembling the elements to get the stiffness matrices for the structure, and obtaining equilibrium equations for the whole system follow the standard procedure of the finite element method.

For dynamic analyses, such as earthquake

problems, the equilibrium equations are solved for each time step of a step-by-step solution process.

6. Results

Based on the macro element described above, a program was developed in Mathcad environment for the nonlinear analysis of *CWR* tracks. Geometric and material nonlinearities can be considered for the analysis of large deformation and buckling of the track. The validity of the program was verified by comparing its results with known solutions [19-23] of axial and lateral buckling of beams, Figures (2) and (3). The properties of the section for these problems were the same as those of Table (1). For all these cases with three elements the results were within 1% of the exact solutions. As we can see from Figures (2) and (3) for more complex displaced shapes more elements are needed for convergence.

Results of the parametric investigations for axial and lateral buckling of the track are described below.

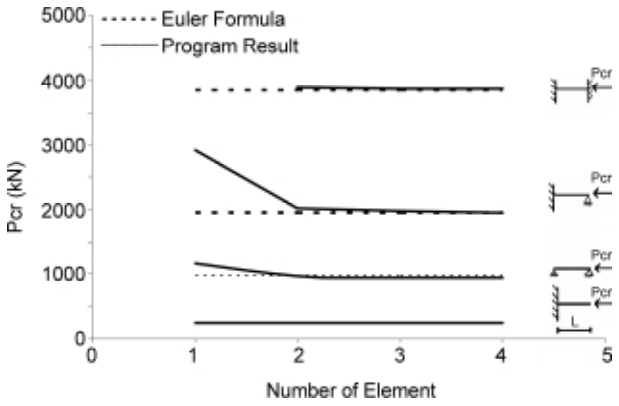

Figure 2. Verification of the critical axial load obtained by the FE solution.

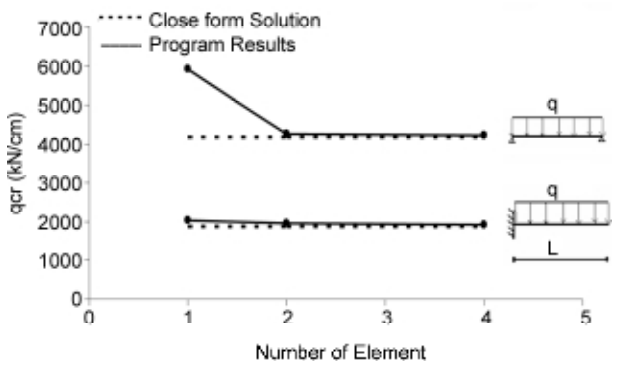

Figure 3. Verification of the critical lateral load obtained by the FE solution.

Table 1. Properties of the rails and ties used in the model.

Rail Type:	**UIC54**
Modulus of Elasticity (N/m^2)	2.1×10
Cross-Section Area (m^2)	6934×10^{-6}
Moment of Inertia I_y (m^4)	2346×10^{-8}
Moment of Inertia I_z (m^4)	417×10^{-8}
Weight Per Unit Length (N/m)	544.3
Coefficient of Thermal Expansion ($m/m/°C$)	0.0000115
Tie Type:	B58
Length (m)	2.4
Mass (kg)	250
Spacing (m)	0.6

7. Axial Buckling of the Track

One of the main problems of railroads is axial buckling of the track because of large temperature variations, and tractive or braking forces of locomotives. Earthquakes do not appear to produce significant increases in the axial force of the track. However, they can reduce the lateral resistance of the track substantially [4, 5, 6, 24], making it vulnerable to instability.

The modes of buckling appear to be different for homogeneous and inhomogeneous tracks. The major parameters affecting the axial buckling of the track are lateral resistance of the ballast and flexural resistance of the rail. To evaluate the effect of these parameters on the critical load, a homogeneous track was modeled first with a sufficient number of macro elements (100 elements) over an adequate length of the track (60m). This model was for *UIC*54 rails and *B*58 ties, which are common in the Iranian Railroads. Table (1) gives the properties of these rails and ties.

The lateral resistance of the track is possibly [25] the most important parameter regarding track stability. An earthquake can easily reduce the lateral resistance of the ballast to half its original strength or less by shaking the base of the track. Figure (4) shows the variation of the critical axial load with lateral resistance of the track. The length of the track, over which buckling takes place, is indicated on the right-hand side of this figure. This length is reduced by increasing lateral resistance. The variation of buckling length, in terms of the lateral resistance of the track, is depicted in the lower curve. This diagram was fitted by an exponential function leading to the following general expression for the buckling length in terms of the stiffness of

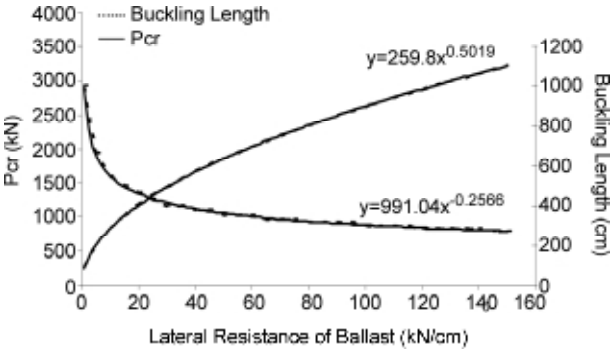

Figure 4. Variation of the critical load with the lateral resistance of ballast, and the associated buckling length.

the rail, EI, and lateral resistance of the ballast, κ,

$$l = 3.2\sqrt[4]{\frac{EI}{\kappa}} \tag{15}$$

Variation of the buckling load with lateral resistance is depicted by the upper curve of Figure (4). In a manner similar to that of buckling length a curve is fitted to the results of the buckling load and when expressed in terms of the rail bending stiffness and lateral track resistance, becomes:

$$P_{cr} = 2\sqrt{EI\kappa} \tag{16}$$

As we can see, the critical load is increased with increasing lateral resistance. This expression is the same [26] as the one derived by assuming a sinusoidal buckling shape. That is, for homogeneous tracks the assumption of a sinusoidal buckling shape, commonly used in practice, is correct. In reality, though, a different buckled shape [3, 6] is observed. In most cases, such as that of Figure (5), the buckled shape is different from sinusoidal. This appears to be due to inhomogeneity along the length of the track.

Figure 5. Photograph of a buckled track from www.modernghana.com/news/305521/1/earthquake-twists-railway-tracks.html.

To investigate this discrepancy, sections of track with varying values of reduced resistance have been instituted along the length of the track and the results obtained are shown in Figure (6). In this figure α is the fraction by which lateral resistance of a portion of the track is reduced. When the total lateral resistance of the track is lost over five ties, the buckling load is decreased by some 45%. Other scenarios may be deduced from Figure (6).

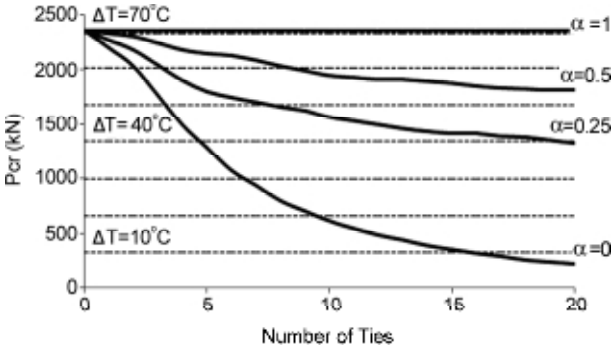

Figure 6. Effect of a series of damaged ties on the critical axial load of the track.

8. Lateral Buckling of the Track

The more common problem encountered in the operation of railroads is probably due to lateral buckling of the track. Lateral buckling, a common problem with deep beams, may occur in rails as well, even though the rail section is not deep. This is because of the lateral force, L, exerted on the head of the rail at the contact point of the wheel and the rail. This force, when it is a large percentage of the vertical load of the wheel, V, can cause a significant lateral deformation of the rail head. Along with the compression force in the rail head, the lateral force may induce instability. This process, called rail overturning in the railroad terminology, will result in the wheel getting off the rail and causing derailment of the train. Obviously, the greater the L/V ratio, the more likely is derailment. Research [27] has indicated that the ratio L/V of about 0.64 can result in derailment when the rail restraint is damaged. The source of lateral force may be the centrifugal effect in curves, coupler forces, wheel creep forces and irregularity in the track geometry. Vertical forces are due to vehicle weight, as well as unbalanced forces in curves, coupler

forces, track geometry and braking and acceleration of locomotives.

Resistance to this type of instability is dependent on bending and torsional stiffness of the rail, lateral resistance of the ballast and torsional resistance of the rail pads. In order to evaluate the lateral-torsional capacity of the track, a model consisting of macro elements was loaded by concentrated lateral and vertical loads, equivalent to the train loads. Torsional loads were induced by the eccentricity of the vertical and horizontal wheel loads. Figure (7) shows the variation of the critical load with lateral resistance of the ballast.

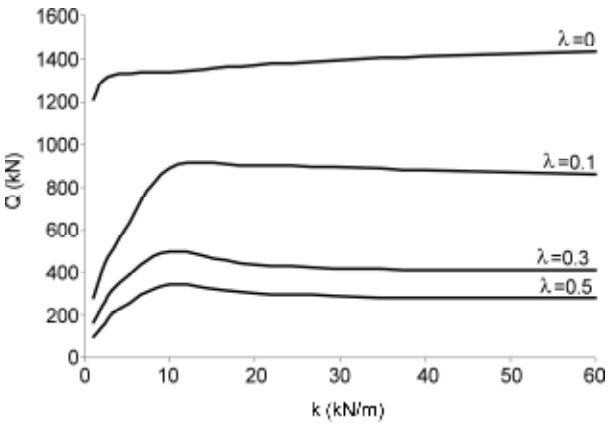

Figure 7. Effect of the reduction in ballast resistance on the lateral-torsional stability of the track.

In this figure, Q is the vertical load and λ is the ratio of the lateral to vertical load. For small values of lateral resistance of the ballast, κ, the critical load varies greatly with this parameter. However, beyond a minimum value ($1 kg/cm$ for the track considered) the critical load is unaffected by κ. This is akin to the lateral bracing of deep beams against lateral-torsional buckling. Most codes require the braces to resist a force equal to about 2% of the axial force in the compressive part of the beam section.

9. Combined Effects of Temperature Increase and Earthquake

The formulation described above can be used for investigating the effects of earthquakes with or without other effects, such as that of temperature change. One parameter which is absent in the above formulation is the ballast shear transfer. This effect was investigated using the $3D$ model of Figure (8), with the stiffness and mass properties of track components. This effect was found to be insignificant.

This model was also used as a check for finding the axial load due to earthquakes. Figure (9) shows the axial load induced by Tabas earthquake record with different *PGA's*.

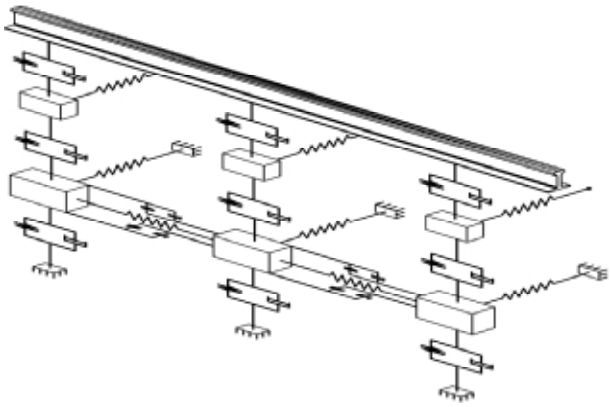

Figure 8. 3D model of track Including shear transfer of ballast.

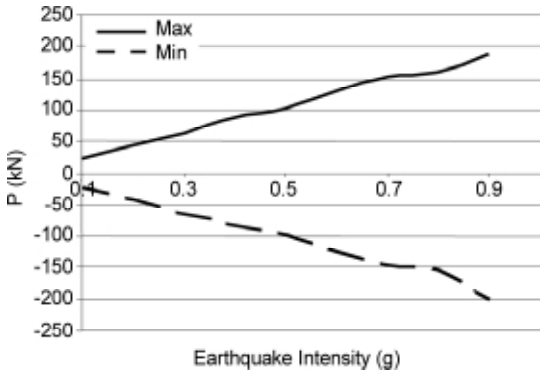

Figure 9. Axial force due to Tabas earthquake with different intensities.

For the actual Tabas earthquake ($PGA = 0.9g$) the axial load thus obtained is about 20%, when compared with the axial load induced by a $40^{o}C$ temperature change, Figure (10). Such temperature changes are not uncommon in most regions of Iran. Therefore, even for a track with an average lateral resistance of $8 kN/m$, the total axial load is about $1600 kN$. The actual buckling load for such a track is $3200 kN$, apparently still a safe situation, if the lateral resistance of the track remains intact. However, because of the lack of cohesiveness of ballast, the devastating effect of an earthquake is the loss of ballast resistance it can cause. Figure

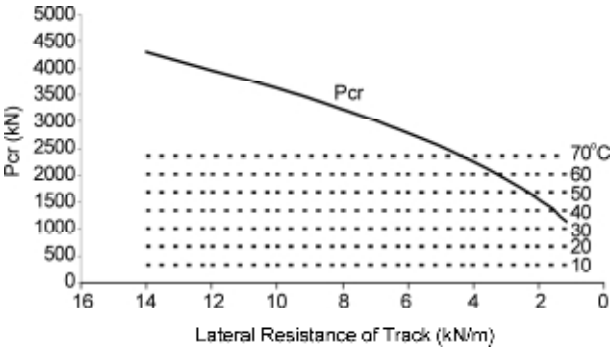

Figure 10. Buckling capacity versus lateral resistance. This may be reduced because of earthquake and thermal effects.

(10) shows that when most of the resistance of the ballast is lost, the buckling capacity is only about 1000*kN*, and hence a very unsafe situation.

Therefore, a combination of a high-temperature change and earthquake can be critical. For this reason when a segment of the track is subjected to an earthquake, before retamping the ballast, train speed should be reduced to avoid derailments.

10. Conclusions

Many train derailments are due to the axial or lateral buckling of railroad tracks. These phenomena were examined in this study by means of a macro element, and parametric studies were conducted in order to determine the effects of the different track parameters on the instability as well as the effect of earthquakes. The following conclusions can be drawn from the results obtained.

In many of the past studies of the axial buckling of the track, a simple sinusoidal shape has been assumed for the deformed track. This assumption is valid only if the track properties are homogeneous along its length. For a structure such as a railroad track, with its significant length, it is not quite possible to have homogeneous properties along its full length. Local inhomogeneity can cause buckling at a lower load and with a different mode shape than sinusoidal. By specifying lower lateral strengths for parts of the track buckling shapes similar to those documented in the field are obtained.

Similar to braces for lateral buckling of beams, a minimum lateral resistance is required to prevent instability. Beyond that value, the buckling capacity for a given track with its stiffness properties remains constant. Therefore, a minimum maintenance program for keeping the track from losing its lateral resistance may go a long way in preventing derailments.

The increase in the axial load due to earthquakes does not seem to be significant when compared with the axial load due to thermal effects and tractive and braking forces of locomotives. However, the effect of earthquake can be critical on the axial and lateral instability of the track, because of the substantial reduction it can cause in the lateral resistance of the track by shaking the ballast bed.

References

1. William, G. and Byers, P.E. (2004). "Railroad Lifeline Damage in Earthquakes", *13 World of Conference on Earthquake Engineering*, Vancouver, B.C, Canada, Paper No. 324.

2. Kerr, A.D. (1976). "The Effect of Lateral Resistance on Track Buckling", Rail Int., **1**, 30-38.

3. Kerr, A.D. (1978). "Thermal Buckling of Straight Track; Fundamentals, Analyses, and Preventive Measures", FRA/ORD-78/49, Washington, DC.

4. Sato, S. (1978). "Lateral Ballast Resistance and Stability of Track in Earthquake", Quarterly Reports, RTRI, **11**(1).

5. Sato, S. (1988). "Buckling Stability of Railway Track in Earthquake", *Proc. Ninth World Conference on Earthquake Engineering*, **VI**, Tokyo-Kyoto, Japan.

6. Grissom, G.T. and Kerr, A.D. (2006). "Analysis of Lateral Track Buckling Using New Frame-Type Equations", *International Journal Mech. Sciences*, **48**, 21-32.

7. Lim, N.H., Park, N.H., and Kang, Y.J. (2003). "Stability of Continuous Welded Rail Track", *Computers and Structures*, **81**, 2219-2236.

8. Lim, N.H., Han, S.Y., and Kang, Y.J. (2008). "Parametric Study on Stability of Continuous Welded Rail Track- Ballast Resistance and Track Irregularity", *Int. J. Steel Structures*, **8**, 171-181.

9. Kish, A., Samavedam, G., and Jeong, D. (1982) "Analysis of Thermal Buckling Tests on U.S. Rail Roads", FRA/ORD-82/45, Washington, DC, USA.

10. Kish, A., Samavedam, G., and Jeong, D. (1985). "Influence of Vehicle Induced Loads on the Lateral Stability of CWR Track", FRA/ORD-82/45, Washington, DC, USA.

11. Samavedam, G., Kish, A., and Jeong, D. (1983). "Parametric Studies on Lateral Stability of Welded Rail Track", DOT, FRA-ORD-93/26, Washington, DC, USA.

12. Samavedam, G., Kish, A., Purple, A., and Schoengart, J. (1993). "Parametric Analysis and Safety Concepts of CWR Track Buckling", DOT/FRA/ORD-93/26, Washington, DC, USA.

13. Samavedam, G. (1979). "Buckling and Post Buckling Analysis of CWR in the Lateral Plane", Technical Note TN-TS-34, British Railway Board.

14. Esveld, C. and Hengstum, L.A. (1988). "Track Stability in Tight Curves", *Rail Int.*, **12**, 15-20.

15. El-Ghazaly, H.A., Sherbourne, A.N., and Arbabi, F. (1991). "Strength and Stability of Railway Tracks-II, Deterministic, Finite Element Stability Analysis", *Computers Structures*, **39**(1/2), 23-45.

16. Jackson, J.E., Bauld, N.R., Ramesh, M.S., and Menon, S.C. (1988). "A Superelement for Lateral Track Deformation", APPL Mech. Rail Transport Symposium.

17. Ramesh, M.S. (1985). "A Nonlinear Finite Element Approach to the Analysis of Lateral Thermal and Mechanical Buckling of Railroad Tracks", Master Thesis, Clemson University.

18. Arbabi, F. (1976). "Variational Formulation of Rail Overturning and a Finite Element Solution Technique", *Transportation Conference*, Los Angeles, CA.

19. Bleich, F. (1952). "Buckling Strength of Metal Structure", McGraw Hill.

20. Barsoum, R.S. and Gallagher, R.H. (1970). "Finite Element Analysis of Torsional and Torsional-Flexural Stability Problems", *Int. J. Numerical Methods in Engineering*, **2**, 335-352.

21. Bazant, Z.P. and Cedolin, L. (1991). "Stability of Structures", Oxford University Press, 373p.

22. Timoshenko, S.P. and Gere, J.M. (1961). "Theory of Elastic Stability", McGraw-Hill.

23. Chen, W.F. and Lui, E.M. (1987). "Structural Stability: Theory and Implementation", Prentice-Hall.

24. Mura, S. (1996). "Deformation of Track and the Safety of Train in Earthquake", Quarterly Reports, RTRI, **37**, No.3.

25. Kabo, E. (2006). "A Numerical Study of Lateral Ballast Resistance in Railway Tracks", *Proc. IMech., Part F: J. Rail and Rapid Transit*, **220**(4), 425-433.

26. Sung, W.P., Shih, M.H., Lin, C.I., and Go, C.G. (2005). "The Critical Loading for Lateral Buckling of Continuous Welded Rail", *J. Zhejiang University Science*, **6A**(8), 878-885.

27. Loumiet, J.R. and Jungbaure, W.G. (2000). "Train Accident Reconstruction and FELA Railroad Litigation", Forth Edition, Lawyers & Judges Publishing Company.

Notations

A: Area of the cross-section of the rail

A, b: Distance of the vertical and horizontal loads from shear center

c, d: Distances of rail centroid and added mass center from the shear center

e: Eccentricity of the axial load

E, G: Elastic and shear moduli of the rail

h: Distance of the lateral supports from shear center

I_p: Polar moment of inertia

I_y, I_z: Moments of inertia about y- and z-axes

J: Torsion constant

k_1, k_2, k_3: Torsional, lateral and vertical resistances of ballast

K_1, K_2, K_3, K_4: Stiffness matrices

$K_{s2}, K_{s3}, K_{s4}, K_{s24}, K_{s42}$: Submatrices of Stiffness

$K_{g2}, K_{g3}, K_{g4}, K_{g24}, K_{g42}$: Submatrices of axial geometric stiffness matrix

$K_{gw24}, K_{gw34}, K_{gw4}, K_{gw23}, K_{gw32}$: Submatrices of lateral geometric stiffness matrix

m_r, m_a: Mass of rail and added mass of other track components

M, N: Shape functions for axial and lateral defor-

mations

M_x: Torque about *x*-axis

$M_{y1}, M_{y2}, M_{z1}, M_{z2}$: Concentrated moments at start and end of element about y and z-axis

P: Axial load

$P_y, p_y, P_{1y}, P_{2y}, P_z, p_z, P_{1z}, P_{2z}$: Load vectors for the horizontal concentrated and distributed loads in the y and z -directions

Q: vertical load applied on the rail

$Q_{y1}, Q_{y2}, Q_{z1}, Q_{z2}$: Shear force at the start and end of element in the horizontal and vertical directions

r_{st}, R_{st}: Displacement and load vectors for the structure

s, S: Displacement and load vectors for element, location of shear center

$\mathbf{s}_1$, $\mathbf{s}_2$, $\mathbf{s}_3$, $\mathbf{s}_4$: Displacement vectors in the *x*-*y*- and *z*-directions, and rotation vector

u_i: Nodal displacements in the x -direction

u_1, u_2: Axial displacements at the start and end of element

U_e, U_s: Elastic energies of the rail and support springs

v, u: Displacements in the *y*- and *z*-directions

v_c, v_g, v_t: Lateral displacement of rail centroid, ground and total displacement

v_i: Nodal displacements in the y-direction

V_p, V_w: Potential energy of axial and lateral loads

V_{w1}, V_{w2}: Potential energies of lateral loads, corresponding to displacements and the flexural-torsional actions

w: Displacement in the z- direction

W_z, W_y: Horizontal and vertical loads, acting at distances a and b (in the vertical direction) from shear center

X: Property of the track section

z_0: Coordinate of shear center

α: Percentage reduction in the lateral resistance of the ballast

β: Rotation about the x-axis

$\delta\Pi, \delta U_e$: Variations of total and elastic energies

δU_s: Variation of energy of the support

$\delta V_p, \delta V_w$: Variation of potential energy of axial and lateral loads

κ: Lateral resistance of ballast

λ: Ratio of lateral to vertical loads

θ_{xi}: Nodal rotation about the *x*-axis